Available online www.jsaer.com

***Journal of Scientific and Engineering Research*, 2017, 4(6):15-26**

Research Article

ISSN: 2394-2630
CODEN(USA): JSERBR

Study of $Fe_{60}Cu_{40}$ Solid Solution Obtained By Attritor Ball Milling

Abdel Monem M. Shamah[1], Mohamed M. El-Desoky[2], Farid F. Hanna[1], Peter N.G. Ibrahim[1]*, Noor A. Ibrahim[1]

[1]Math and Sciences department, Faculty of Petroleum and Mining Engineering, Suez University, Suez, Egypt
[2]Physics department, Faculty of Science, Suez University, Suez, Egypt

Abstract Single phase f.c.c. $Fe_{60}Cu_{40}$ solid solution was successfully obtained by attritor ball milling after 10 hours of milling. The formation of this solid solution after this short time of milling spots the light on the advantage of attritor as a powerful tool of mechanical alloying, capable of providing sufficiently high energy during the milling process. The formed f.c.c. $Fe_{60}Cu_{40}$ solid solution has a grain size in the nano-scale (about 10 nm), and a lattice parameters expanded with respect to that of pure f.c.c. Cu. The high temperature annealing of the formed f.c.c. $Fe_{60}Cu_{40}$ solid solution results in the decomposition of the solid solution and in the separation of phases. The formed f.c.c. $Fe_{60}Cu_{40}$ solid solutions were found to be ferromagnetic, which confirms the existence of f.c.c. Fe atoms in these solid solutions in magnetic state with non-zero value of magnetic moment. Our calculations of magnetic moment per Fe atom gave a value of 1.465 μ_B for the $Fe_{60}Cu_{40}$ sample after 10 hours of milling, and 1.373 μ_B after 20 hours of milling. These values are discussed in light of the possibility of coexistence of γ-Fe in two magnetic states (HS and LS) in these solid solutions.

Keywords Fe-Cu, Mechanical alloying, Attritor, Magnetic properties

Introduction

According to the equilibrium phase diagram of the Fe-Cu system [1], It is known that, copper has a f.c.c. crystalline structure, iron at room temperature has a b.c.c. crystalline structure (known as γ-Fe phase), which is transformed when heated to temperature 1183K to a f.c.c. crystal structure (known as γ-Fe). The γ-Fe is a high temperature phase and is not stable at room temperature. Both Fe and Cu have negligible mutual solid solubility in equilibrium at temperatures below 700 ^oC. The Fe-Cu system has a large positive energy of mixing ($\Delta H_f \sim +$ 13 kJ/mol) [2].

Recently, the mechanical alloying (MA) appeared as a powerful tool of preparation of supersaturated solid solutions between elements immiscible, or with limited solubility, in the equilibrium conditions, such as the Fe-Cu system, in which the formation of supersaturated solid solutions was reported in the whole range of iron and copper compositions [2-8].

In the process of mechanical alloying (also known as ball milling), repeated mechanical deformations, cold welding and fracture of the alloyed powder particles take place, due to their repeated collisions with steel balls and vial. The process of alloying takes place due to the energy provided by these collisions [9]. Different types of mills are used in the process of mechanical alloying [9-10], for example, the vibratory ball mill, the planetary ball mill and the attritor (which have been used in the present work).

The formed Fe_xCu_{100-x} solid solutions can have a b.c.c. or f.c.c. crystalline structure, or even a mixture of both of them, in dependence on the iron and copper concentrations. In the published data, there is not complete agreement about the boundaries between the regions of existence of these different types of crystalline

structures, which seems to be dependent on the method of preparation of these solid solutions, and even on the parameters of preparation [8, 11]. According to many of the published articles, concerning the formation of Fe_xCu_{100-x} solid solutions by mechanical alloying, the f.c.c. phase is formed for iron concentration $x \leq 60$, the b.c.c. phase is formed for $x \geq 80$, while a mixture of both phases is obtained for $60 < x < 80$ [8].

It can be noted, that the formation of f.c.c. Cu(Fe) solid solution by mechanical alloying is considered as an interesting way to stabilize the f.c.c. γ-Fe at room temperature, by substituting it in the Cu-lattice, which has the same f.c.c. crystalline structure, and which has lattice parameter close to that of γ-Fe [12-14]. Since Cu atoms are non-magnetic, the f.c.c. Cu(Fe) solid solutions, formed by mechanical alloying, can be used to test the magnetic properties of f.c.c. γ-Fe at room temperature. It is known that, the γ-Fe, in its equilibrium stability (above 1183K) is also non-magnetic.

To the best of our knowledge, the majority of researches, concerning the formation of Fe_xCu_{100-x} solid solutions by mechanical alloying, used the vibratory ball mill or the planetary ball mill to prepare these solid solutions, while the published data about the Fe_xCu_{100-x} solid solutions, formed by attritor ball mill, are rare. Consequently, this present work is aimed to study the formation of $Fe_{60}Cu_{40}$ solid solution by the attritor ball milling, and to study the microstructure of the formed phase(s). The composition is chosen at the boundary of formation of the f.c.c. phase, according to the published literature, to provide new data, based on the attritor ball mill, that confirm (or disagree with) the previously published data, about this boundary of formation of the f.c.c. phase.

The study of magnetic properties of the $Fe_{60}Cu_{40}$ solid solution, prepared by the attritor ball milling, is another objective of the present work. It was reported [5,6,15,16] that, most of the obtained Fe_xCu_{100-x} solid solutions are ferromagnetic, in exception of those solid solutions very rich in copper, which are paramagnetic. The appearance of ferromagnetism in the f.c.c. Fe_xCu_{100-x} solid solutions is very interesting, since both Cu and f.c.c-Fe are non-magnetic [14]. The ferromagnetism of these f.c.c. Fe_xCu_{100-x} solid solutions was discussed [12-14], in the light of the model of Weiss [17], according to which, the γ-Fe can exist in two different spin-electronic states; known as "low spin-low volume" state (LS) with lattice parameters around 3.5 Å, and "high spin-high volume" state (HS) with lattice parameters above 3.6 Å. The value of magnetic moment per iron atom in the LS state is estimated to be below 1 μ_B, while for HS state can reach values over 2.5 μ_B. Therefore, it was pointed, that the magnetic state of γ-Fe depends on the lattice parameter of the crystalline structure, in which γ-Fe atoms are stabilized (and hence depends on the change of the crystalline field inside the formed solid solutions).

Experimental Procedure

Iron powder (of purity 99%) and copper powder (of purity 99.9%) have been weighted to obtain the desired composition $Fe_{60}Cu_{40}$, and placed in high energy attritor ball mill. Several samples $Fe_{60}Cu_{40}$ have been prepared, after different milling times. The powders were treated with hard steel balls at different milling times with the balls to powder ratio equals to 20:1, and rotation speed 500 rpm. The milling process was performed in continuous argon atmosphere to prevent the oxidation of the samples.

XRD was performed using D5000 powder diffractometer using Cu Kα radiation (wavelength $\lambda = 0.15406$ nm) with a nickel filter at 40 kV and 30 mA. The diffractometer was operated within range of $10° < 2\theta < 100°$ with one second step-time and 0.05 degree step-size. Diffraction signal intensity throughout the scan was monitored and processed with DIFFRAC plus software. Scanning electron microscope images of the $Fe_{60}Cu_{40}$ sample, after 10 hours and 20 hours of milling were obtained by quanta fei 250 Scanning Electron Microscope.

To investigate the thermal stability of the obtained solid solution, sample $Fe_{60}Cu_{40}$, after 20 hours of milling, was compressed in tablets, annealed at temperatures 200C, 300C and 400C for one hour, followed by cooling in furnace. The magnetic hysteresis loops of the obtained $Fe_{60}Cu_{40}$ samples, after 10 hours and 20 hours of milling, were measured by a Vibrating Sample Magnetometer Lake Shore model 7410 (USA) at different temperatures (100K, 150K, 300K and 450K).

Results and Discussion

X-ray diffraction patterns

X-rays diffraction patterns of the $Fe_{60}Cu_{40}$ sample after different milling times are represented in fig 1 and fig 2. The mechanical alloying process of the $Fe_{60}Cu_{40}$ powder resulted in the reduction of the intensities of x-ray

diffraction peaks and their broadening, as seen in fig 1 and 2, which is attributed to the reduction of the grain size, and also to the introduction of internal strain during the milling process. According to the x-ray diffraction pattern, the formation of new phases were not detected up to 30 hour milling, but it was observed, that the peaks of b.c.c. iron disappeared after 10 hours of milling. Also a shift of the Cu peaks toward the smaller 2θ angles was observed (see fig 2). The disappearance of the Fe peaks and the shift of the Cu peaks gave an indication of the formation of solid solution of Fe in Cu matrix (Cu(Fe) solid solution), which took place, according to our results, after 10 hours of milling.

As seen in fig 1 and fig 2, the diffraction peaks of f.c.c. Cu are shifted toward the smaller 2θ angles with increasing the milling time, which corresponds to the expansion of f.c.c. lattice parameters during the formation of Cu(Fe) solid solution, due to the substitution of Cu atoms by Fe atoms. It should be mentioned here, that the atomic radius of copper (r_{Cu} = 1.28 Å) is greater than that of iron (r_{Fe} = 1.26 Å) [18], consequently, the expansion of lattice during the formation of f.c.c. Cu(Fe) solid solution can't be explained by the difference in atomic radii of Fe and Cu atoms, but it was suggested that, this increase of lattice parameters of the f.c.c. phase is most likely attributed to magnetovolume effects (The f.c.c. phase becomes ferromagnetic, which expands the unit-cell volume, as compared to the corresponding paramagnetic material, because of the magnetovolume effect) [19-21].

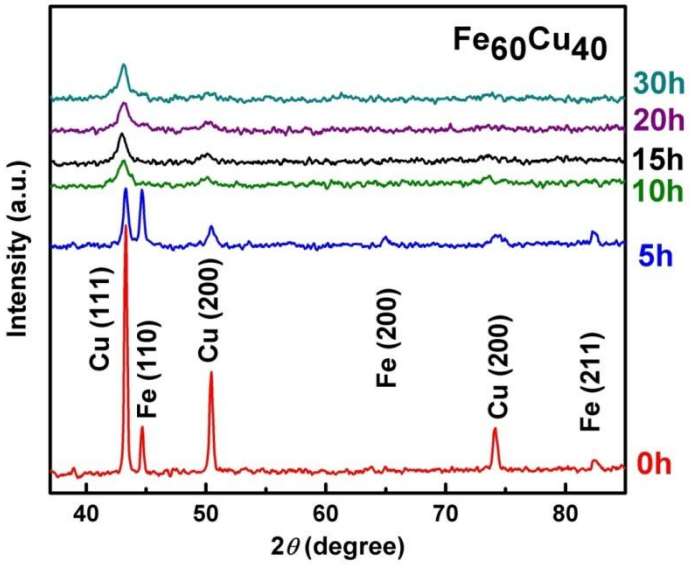

Figure 1: X-rays diffraction patterns of the $Fe_{60}Cu_{40}$ sample after different milling times

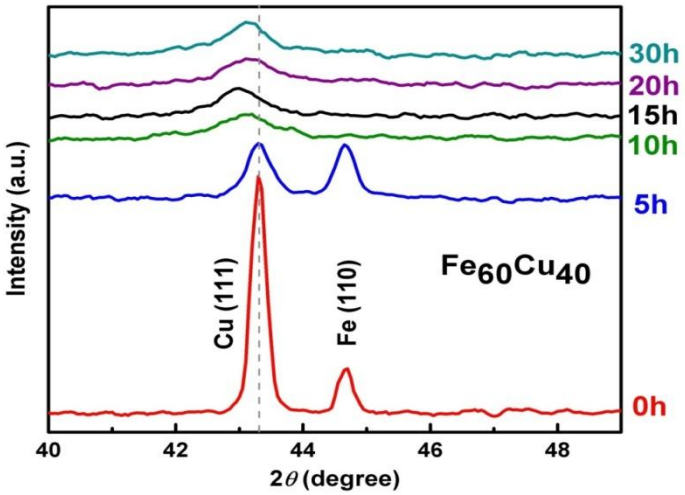

Figure 2: a detailed view of the main peak of b.c.c. Fe and f.c.c. Cu in the x-ray diffraction patterns of the $Fe_{60}Cu_{40}$ powder after different milling times.

The variation of the lattice parameter (*a*) of the f.c.c. phase with increasing the milling time of the $Fe_{60}Cu_{40}$ sample, calculated from the peak position of the main Cu peak in the x-ray diffraction patterns, is represented in fig 3.

It can be suggested that, the dependence of lattice parameter (*a*) on milling time, as shown in fig 3, seems to pass by two different stages during the milling of the $Fe_{60}Cu_{40}$ sample. The first stage, up to 10 hours of milling, is characterized by an increase of the lattice parameters. By the end of this stage, all the iron atoms are introduced inside the copper f.c.c. lattice, and a solid solution of Fe in Cu lattice is formed. The second stage, observed for further milling time, can be characterized as a steady state stage, in which the change in lattice parameters is very small, as compared with the first stage. In this second stage, no more Fe atoms are introduced inside the Cu lattice, therefore, the lattice parameters do not continue to increase, but it can be suggested that, in this stage the Fe atoms, which already exists inside the Cu lattice, continue to diffuse inside the f.c.c. lattice to occupy energetically preferred positions, and to complete the alloying process to atomic level.

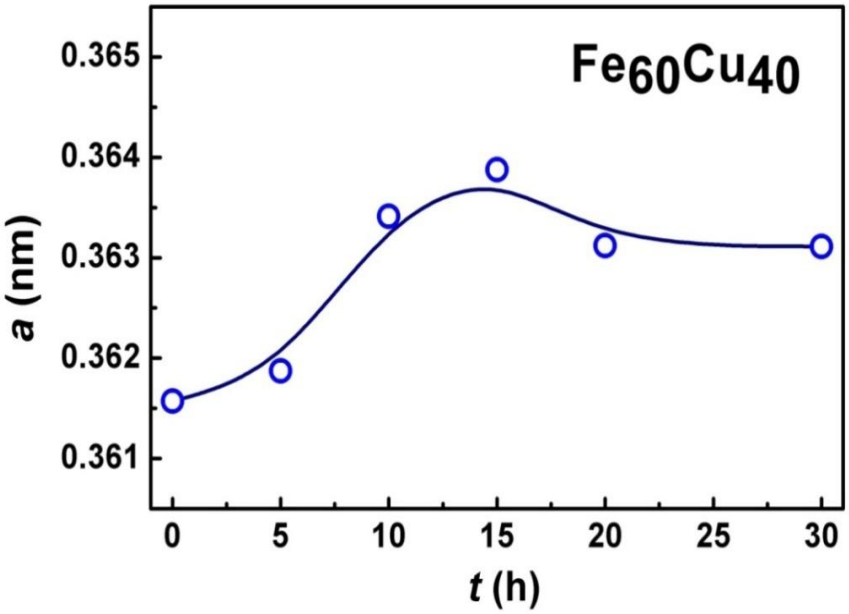

Figure 3: The variation of the lattice parameter (a) of the f.c.c. phase with increasing milling time of the $Fe_{60}Cu_{40}$ powder.

It can be noted that, this trend (dependence) of lattice parameter of the formed Cu(Fe) solid solution on milling time is in good agreement with previously published data [8, 21-23], but it should be mentioned also, that, there is some kind of disagreement in these publications about the rate of expansion of lattice parameters and the milling time required to reach the steady state stage, which can be explained by the dependence of these parameters on the milling parameters and the amount of energy transferred to the alloyed powder.

It should be also mentioned, that according to our results, obtained on attritor ball mill, the formation of f.c.c. Cu(Fe) solid solution was achieved after 10 hour of milling, which is considered as one of the shortest milling time reported for the formation of solid solution in this system, when comparing with previously published data. Consequently, our results spot the light on the advantage of the attritor ball mill, with the milling parameters indicated in the present work, as a tool of preparation of solid solution on the Fe-Cu system, due to its capability to provide high rate of energy transfer to the alloyed powder, necessary to achieve the formation of solid solutions in minimum interval of milling time.

The grain size of the formed f.c.c. Cu(Fe) solid solution was estimated from the x-ray diffraction pattern by using Scherrer's formula [24], $D = 0.9\lambda / B(2\theta) \cos(\theta)$, where λ is the wavelength of the x-ray beam (in the present study $\lambda = 0.15406$ for Cu K_α radiation), and $B(2\theta)$ is the FWHM of the diffraction peak located at angular position 2θ [corrected for instrumental broadening, by using the formula $B^2(2\theta) = B^2_{measured}(2\theta) - B^2_{instrumental}(2\theta)$]. Scherrer's formula was applied to the main peak of the f.c.c. phase. It should be noted here,

that the complete Williamson Hall formula, which is used to evaluate both the grain size and microstrain, was not applicable in our x-ray patterns, due to the considerable broadening of the diffraction peaks and their reduction in intensity, which make it so difficult, except for the main peak, to separate accurately the peak from the background for accurate determination of FWHM. Therefore, the values of grain size, calculated by Scherrer's formula, can be taken only as a lower limit of the grain size, since the broadening due to the internal strain is not included in calculations.

The evolution of the grain size of the f.c.c. Cu(Fe) solid solution with the increase of milling time is shown in fig 4. As seen in fig 4, increasing the milling time leads to the decrease of the grain size of the f.c.c. Cu(Fe) solid solution to about 10 nm after 10 hours of milling. For further milling the grain size is weakly changes, and have nearly steady-state value .The obtained value of grain size confirms the ability of the mechanical alloying (attrition ball mill) to produce nanocrystalline f.c.c. Cu(Fe) solid solutions (with grain size in the nanoscale). These obtained results are in good agreement with the previously published data about the mechanically alloyed Fe-Cu system [3,8,11,25,26].

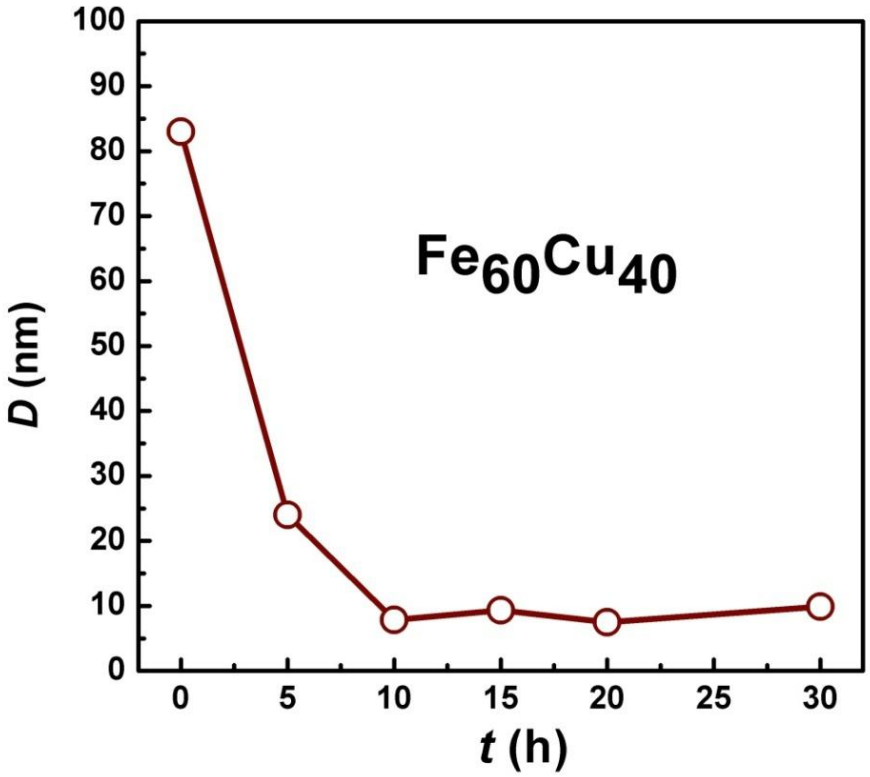

Figure 4: The dependence of the grain size (D) of the f.c.c. phase with on the milling time of the $Fe_{60}Cu_{40}$ powder

Scanning Electron Microscope Images

The scanning electron microscope SEM images of the mechanically alloyed $Fe_{60}Cu_{40}$ sample after 10 hours and 20 hours of milling are presented in fig 5. For comparison, the SEM image of the same sample without milling (zero time) is also presented in fig 5. The sample after 10 and 20 hours of milling has a plate-like morphology, as seen from fig 5, in contrast with the initial sample (before milling) which has a spherical morphology (characteristic for the initial non-milled Fe and Cu particles). The appearance of plate-like morphology in the $Fe_{60}Cu_{40}$ sample after 10 hours and 20 hours of milling is a consequence of the mechanical alloying process, in which successive cold welding, fracture and plastic deformation of the milled powder take place, which in turn causes the flattening of the milled particles, changing their morphology to the plate-like shape.

The size of the mechanically alloyed $Fe_{60}Cu_{40}$ particles, as seen in SEM images, after 10 and 20 hours is estimated to be in the range of some hundreds nanometers. It should be noted here, that this estimated particle size is completely different from the grain (crystallite) size calculated by Scherrer's formula. The mechanically

alloyed particles, as seen in SEM image are the result of agglomeration of a great number of crystallites, which in turn make it not possible to view separate grains by SEM.

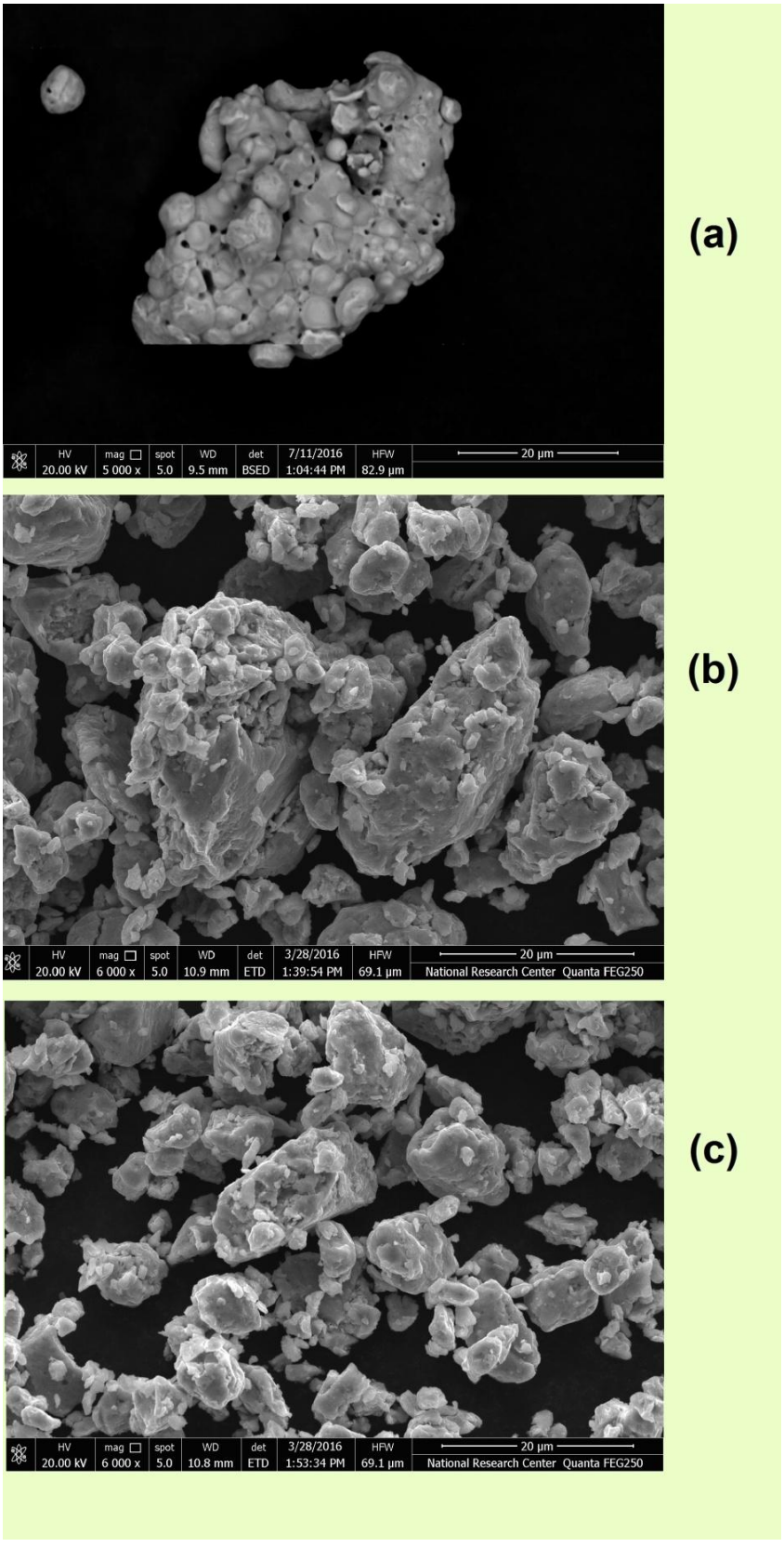

Figure 5: SEM of Fe60Cu40 alloy. (A) Without milling. (B) After 10 hours. (C) After 20 hours

Thermal stability of the $Fe_{60}Cu_{40}$ solid solution obtained by mechanical alloying

To investigate the thermal stability of the $Fe_{60}Cu_{40}$ solid solution obtained by mechanical alloying, the sample after 20 hours of milling were compressed and annealed at temperatures 200C, 300C and 400C for 1 hour at each temperature. The x-ray diffraction patterns, at the 2θ-range around the main peak of the f.c.c. phase, after these heat treatments are shown in fig 6.

As shown in fig 6, with the increase of annealing temperature, the b.c.c. Fe-peak reappeared, and in clearly seen after annealing at temperature 400C. These results show that, the f.c.c. $Fe_{60}Cu_{40}$ solid solution formed by mechanical alloying is not thermally stable, and undergoes a phase separation into b.c.c. Fe and f.c.c. Cu phases. The degree of separation of these phases increases with increasing the temperature of annealing, and become obvious after annealing at temperature 400C.

It can be also noticed, that a shift of the main f.c.c. diffraction peak toward the higher 2θ is observed with the increase of temperature of annealing, as shown in fig 6, which corresponds to the contraction of the f.c.c. lattice. This is easly explained in the light of the separation of the b.c.c. Fe from the f.c.c. lattice, and the return of the lattice parameters of the f.c.c. phase to that of pure f.c.c. Cu.

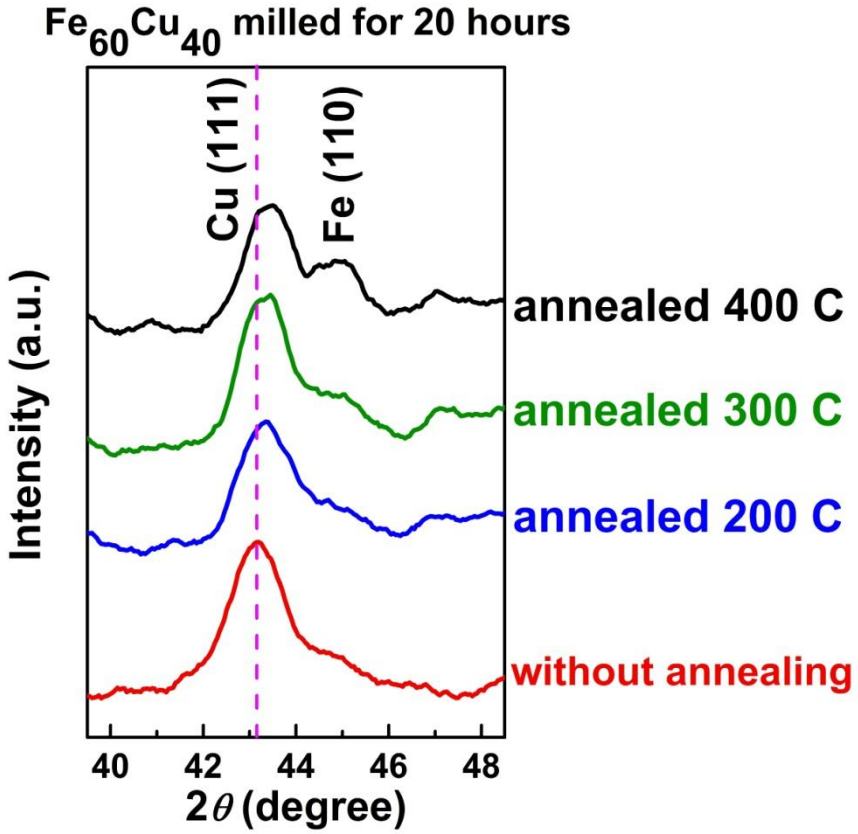

Figure 6: X ray diffraction patterns of the $Fe_{60}Cu_{40}$ solid solution obtained by mechanical alloying for 20 hours, followed by annealing at the indicated temperatures for 1 hour

Magnetic Measurements

The curves of the field dependence of magnetization (hysteresis loops) of the $Fe_{60}Cu_{40}$ sample after 10 hours and 20 hours of milling are shown in fig 7 and fig 8, respectively. The shape of the measured hysteresis loops are characteristic to the existence of ferromagnetic ordering in these $Fe_{60}Cu_{40}$ solid solutions, formed by mechanical alloying.

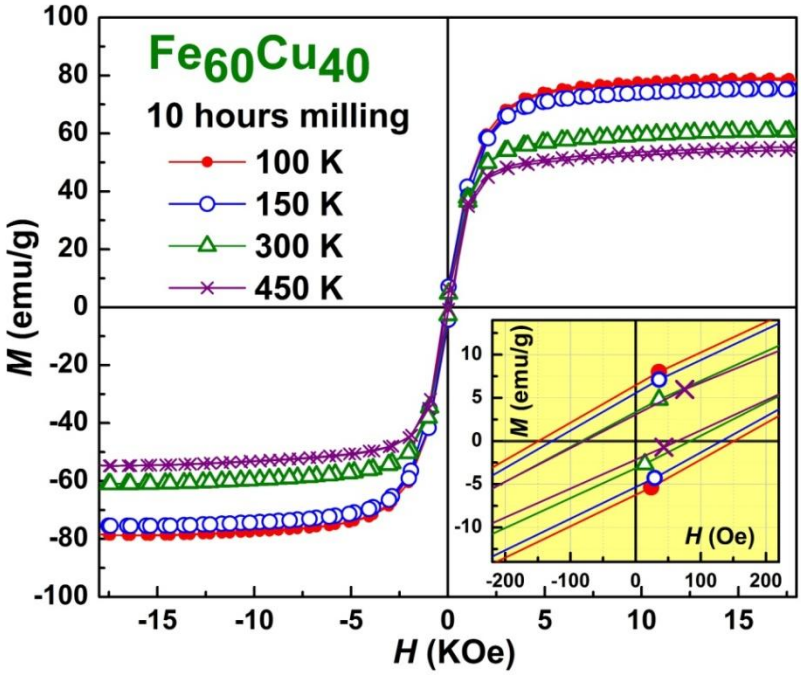

Figure 7: The dependence of magnetization (M) on the intensity of magnetic field (H) for the $Fe_{60}Cu_{40}$ sample after 10 hours of milling

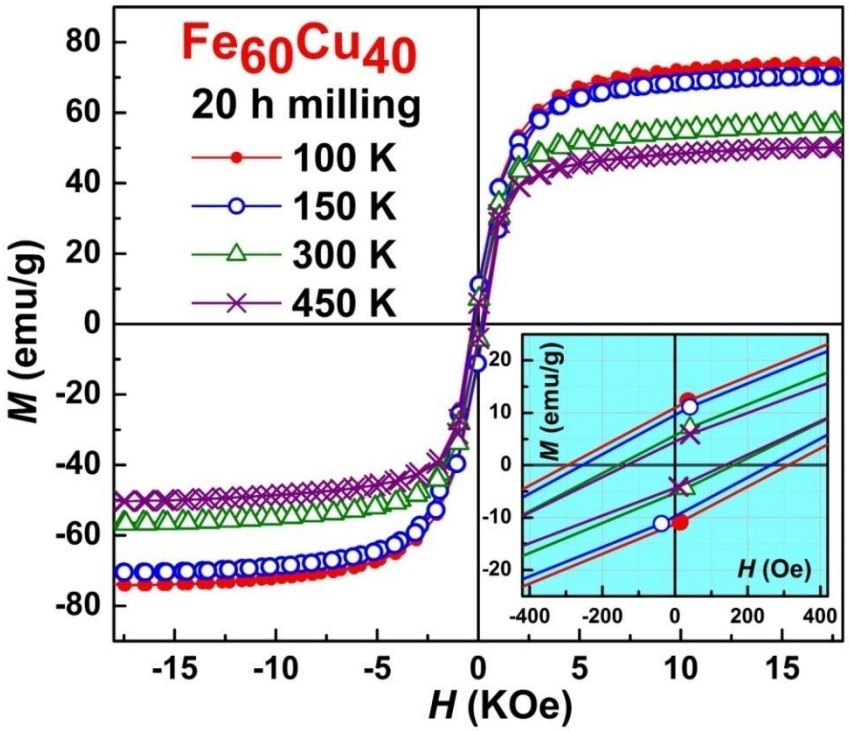

Figure 8: The dependence of magnetization (M) on the intensity of magnetic field (H) for the $Fe_{60}Cu_{40}$ sample after 20 hours of milling

It is interesting, why the mechanically alloyed $Fe_{60}Cu_{40}$ solid solutions show ferromagnetic behavior, while both f.c.c. Cu and f.c.c. Fe (γ-Fe) are non-magnetic. The appearance of ferromagnetism in the f.c.c. Cu(Fe) solid solutions can be attributed, as was discussed in the work of Gorria [12-14], to the existence of γ-Fe in high spin (HS) state in the f.c.c. environment of Cu lattice. Since the lattice parameter of the pure f.c.c. Cu is about 3.615

Å (see fig 3), which is close to that of the γ-Fe in the HS state, therefore it is more favorable for the γ-Fe in the f.c.c. environment of Cu lattice to exist in the HS state, leading to the ferromagnetism of these f.c.c. Cu(Fe) solid solutions, as confirmed our results for the mechanically alloyed $Fe_{60}Cu_{40}$ solid solutions.

From another point of view, our results (in agreement with previously published data) showed, that the substitution of f.c.c. Cu atoms by the f.c.c. Fe atoms during the formation of f.c.c. Cu(Fe) solid solutions resulted in the expansion of the lattice and the increase of lattice parameters (see fig 3). This can be explained by the existence of γ-Fe in its HS magnetic state in these solid solutions, and taking into consideration the magnetostriction effect caused by the change of the magnetic state of γ-Fe, located inside the Cu lattice.

From the hysteresis loops (fig. 7 and 8), it can be seen that, the values of coercivity H_c, remanence M_r and saturation magnetization M_s decrease, as expected, with increasing the temperature, due to the effect of thermal agitation, which opposes the ordering of magnetic moments (tends to their disordering).

To determine the saturation magnetization $M_s(0)$ at nearly 0K, a plot of the $M_s(T)$ as a function of $T^{3/2}$ were performed, in accordance of Bloch $T^{3/2}$ law [$M(T)=M(0)(1-BT^{3/2})$] based on the spin-wave excitation in ferromagnetic materials [15]. The saturation magnetization $M_s(0)$ at nearly 0 K is obtained from the extrapolation of the linear part of the Bloch $T^{3/2}$ plot to T = 0 K, as shown in fig 9. It should be noted, that our experimental data are well fitted by Bloch $T^{3/2}$ law in temperature range up to 300 K, which confirms the existence of ferromagnetic ordering in these samples. The obtained values of $M_s(0)$ are 83.3 emu/g for the $Fe_{60}Cu_{40}$ sample after 10 hours of milling, and 78.1 after 20 hours of milling.

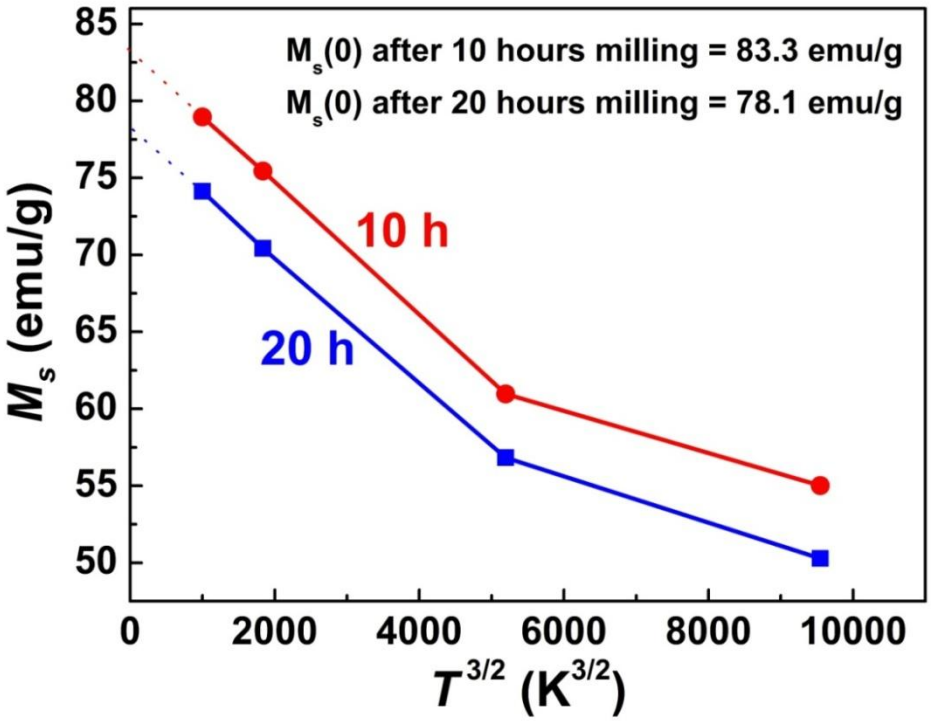

Figure 9: the saturation magnetization as a function of $T^{3/2}$, based on Bloch $T^{3/2}$ law, for the $Fe_{60}Cu_{40}$ sample after 10 hours and 20 hours of milling

From these calculated values of saturation magnetization at zero Kelvin $M_s(0)$ the magnetic moment μ per unit formula ($Fe_{60}Cu_{40}$) can be estimated, by using the relation $\mu = (M_s(0) \times M.W) / (N_A \times \mu_B) = (M_s(0) \times M.W) / 5585$, where M.W is the molecular weight of the unit formula, N_A is Avogadro's number (6.02252×10^{23} $mole^{-1}$) and μ_B is Bohr magneton (9.2732×10^{-21}erg/G). After that, the magnetic moment per iron atom μ_{Fe} can be estimated, assuming a ferromagnetic ordering of magnetic moments and assuming that, Cu atoms have no magnetic moment. In this way, our calculations leaded to a value of magnetic moment per iron atom μ_{Fe} of 1.465 μ_B for the $Fe_{60}Cu_{40}$ after 10 hours of milling, and 1.373 μ_B after 20 hours of milling. The existence of none-zero value of magnetic moment per iron atom accounts for the appearance of ferromagnetism in the

mechanically alloyed $Fe_{60}Cu_{40}$ samples. The values of magnetic moment per Fe atom, as calculated from our magnetic measurements, are in acceptable agreement with some previously published data [3], while other published data gave higher values of magnetic moment per Fe atom (around $2\mu_B$) [2, 27-28]. Our calculated value of magnetic moment per Fe atom is also lower than that, suggested by Weiss model for the γ-Fe in the HS state. It seems that, not all the Fe atoms existing in the f.c.c. Cu-lattice are in high spin state, but some Fe atoms are in low spin state or non-magnetic state, in dependence on the local environment surrounding each atom. The existence of fraction of Fe atoms in non-magnetic state in the mechanically alloyed Fe-Cu system was also suggested by the results of Mossbauer spectroscopy [15], and the coexistence of Fe atoms in two different magnetic state (HS favoring the ferromagnetic coupling and LS favoring the antiferromagnetic coupling] in the mechanically alloyed Fe-Cu system, was confirmed by the results of XMCD [29].

To investigate the effect of milling time on the magnetic characteristics M_r, H_c and M_s of the mechanically alloyed $Fe_{60}Cu_{40}$ sample, the hysteresis loops M(H) at room temperature (T = 300K) of the $Fe_{60}Cu_{40}$ sample after 10 and 20 hours of milling are plotted in fig 10, together with the hysteresis loop of the starting $Fe_{60}Cu_{40}$ sample without mechanical alloying. As seen from fig 10, and also from fig 8, the coercivity and the remanence of the $Fe_{60}Cu_{40}$ sample increases considerably with the increase of milling time. The coercivity increased from about 20 Oe before milling at RT to about 160 Oe after 20 hours of milling at RT, which reached about 305 Oe at T=100K. The increase of coercivity can be attributed to the decrease of grain size and the introduction of micro strain accompanying the mechanical alloying process.

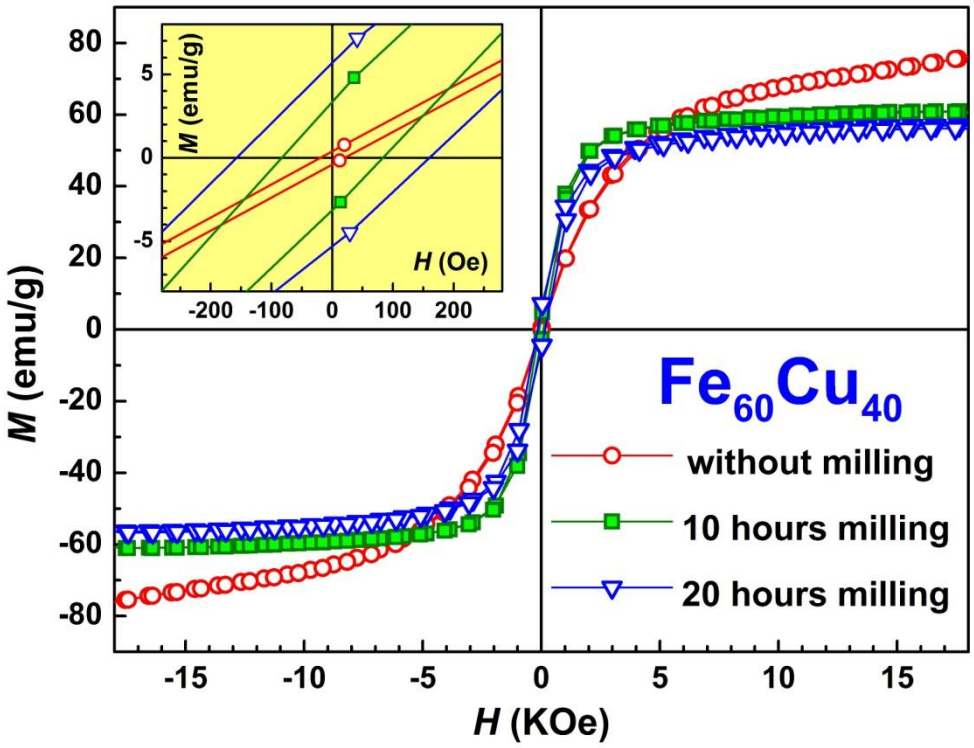

Figure 10: The dependence of magnetization (M) on the intensity of magnetic field (H) for the $Fe_{60}Cu_{40}$ sample without milling and after 10 hours and 20 hours of milling at T = 300 C

It can be also noticed, that the magnetization of the initial $Fe_{60}Cu_{40}$ sample (without mechanical alloying) does not saturate up to an applied magnetic field of 18 KOe, while the mechanically alloyed samples saturate easily in lower magnetic fields, as shown in fig 10. Generally, it is seen that, the magnetization at high magnetic fields tend to decrease with increasing the milling time, which can be related to the change of iron from b.c.c. structure to f.c.c. structure, and the change of magnetic moment of iron atoms, due to the change of their surrounding crystalline field. It can be also noted that, there is a difference in the value of saturation magnetization in the samples after 10 hours and 20 hours of milling, which seems to be related to the change of the value of magnetic moment of Fe atom, and/or the change of fraction of f.c.c. Fe existing in HS state, due to the change of local environment surrounding the Fe atoms.

Conclusions

The main conclusions of the present work can be summarized in the following points:

Single phase nanocrystalline f.c.c. solid solution $Fe_{60}Cu_{40}$ was successfully prepared by attritor ball milling after 10 hours of milling, which confirms the ability of attritor to provide sufficiently high energy during the milling process, resulting in the formation of single phase solid solution after considerably short time of milling, comparable and even better than that reported in the published data by using other tools of mechanical alloying.

The formation of the solid solution $Fe_{60}Cu_{40}$ was accompanied by f.c.c. lattice expansion, compared with that of pure f.c.c. Cu, and which was suggested to be attributed to magnetovolume effects.

The mechanically alloyed $Fe_{60}Cu_{40}$ solid solutions are thermally unstable, and their annealing at relatively high temperature (300 °C, 400 °C) results in the decomposition of the solid solution and in the separation of b.c.c. Fe and f.c.c. Cu phases.

The formed $Fe_{60}Cu_{40}$ solid solutions are found to be ferromagnetic, which confirm the existence of f.c.c. Fe atoms in these solid solutions in magnetic state with non-zero value of magnetic moment. Our calculations of magnetic moment per Fe atom gave a value of 1.465 μ_B for the $Fe_{60}Cu_{40}$ sample after 10 hours of milling, and 1.373 μ_B after 20 hours of milling. These values are discussed in light of the possibility of coexistence of γ-Fe in two magnetic states (HS and LS) in these solid solutions.

References

1. Okamoto, H. (1993). Phase Diagrams of binary iron alloys ASM International. *Materials park, OH*: 131-137.
2. Ma, E., Atzmon, M., & Pinkerton, F. E. (1993). Thermodynamic and magnetic properties of metastable Fe_xCu_{100-x} solid solutions formed by mechanical alloying. *Journal of applied physics*, 74(2): 955-962.
3. Ambrose, T., Gavrin, A., & Chien, C. L. (1993). Magnetic properties of metastable fcc Fe-Cu alloys prepared by high energy ball milling. *Journal of magnetism and magnetic materials*, 124(1-2): 15-19.
4. Gaffet, E., Harmelin, M., & Faudot, F. (1993). Far-from-equilibrium phase transition induced by mechanical alloying in the Cu-Fe system. *Journal of alloys and compounds*, 194(1): 23-30.
5. Ueda, Y., Ikeda, S., Mori, Y., & Zaman, H. (1996). Magnetoresistance and magnetism in Fe-Cu alloys produced by electrodeposition and mechanical alloying methods. *Materials Science and Engineering: A*, 217: 371-375.
6. Ino, H., Hayashi, K., Otsuka, T., Isobe, D., Tokumitsu, K., & Oda, K. (2001). Appearance of ferromagnetism in fcc solid solutions of binary and ternary Fe–Cu-based systems prepared by mechanical alloying technique. *Materials Science and Engineering: A*, 304: 972-974.
7. Wei, S., Yan, W., Li, Y., Liu, W., Fan, J., & Zhang, X. (2001). Structural transitions of mechanically alloyed $Fe_{100-x}Cu_x$ systems studied by X-ray absorption fine structure. *Physica B: Condensed Matter*, 305(2): 135-142.
8. Mojtahedi, M., Goodarzi, M., Aboutalebi, M. R., Ghaffari, M., & Soleimanian, V. (2013). Investigation on the formation of Cu–Fe nano crystalline super-saturated solid solution developed by mechanical alloying. *Journal of Alloys and Compounds*, 550: 380-388.
9. Suryanarayana, C., Ivanov, E., & Boldyrev, V. V. (2001). The science and technology of mechanical alloying. *Materials Science and Engineering: A*, 304: 151-158.
10. El-Eskandarany, M. S. (2015). *Mechanical alloying: nanotechnology, materials science and powder metallurgy*. Elsevier.
11. Jiang, J. Z., Gente, C., & Bormann, R. (1998). Mechanical alloying in the Fe–Cu system. *Materials Science and Engineering: A*, 242(1): 268-277.
12. Gorria, P., Martínez-Blanco, D., Blanco, J. A., Hernando, A., Garitaonandia, J. S., Barquín, L. F., Campo, J. & Smith, R. I. (2004). Invar effect in fcc-FeCu solid solutions. *Physical Review B*, 69(21): 214421.
13. Gorria, P., Martínez-Blanco, D., Blanco, J. A., Pérez, M. J., Hernando, A., Barquín, L. F., & Smith, R. I. (2005). High-temperature induced ferromagnetism on γ− Fe precipitates in FeCu solid solutions. *Physical Review B*, 72(1), 014401.

14. Gorria, P., Martínez-Blanco, D., Iglesias, R., Palacios, S. L., Pérez, M. J., Blanco, J. A., Fernandez, L., Hernando, A., & González, M. A. (2006). Magneto-volume effects in Fe–Cu solid solutions. *Journal of magnetism and magnetic materials*, 300(1), 229-233.
15. Yousif, A., Bouziane, K., Elzain, M. E., Ren, X., Berry, F. J., Widatallah, H. M., Al Rawas, A., Gismelseed, A., & Al-Omari, I. A. (2004). Magnetic Properties of Nanocrystalline Fe_xCu_{1-x} Alloys Prepared by Ball Milling, *Hyperfine interactions*, 156:213-221.
16. Sumiyama, K., Yoshitake, T., & Nakamura, Y. (1984). Magnetic properties of metastable bcc and fcc Fe-Cu alloys produced by vapor quenching. *Journal of the Physical Society of Japan*, 53(9): 3160-3165.
17. Weiss, R. J. (1963). The Origin of the Invar'Effect. *Proceedings of the Physical Society*, 82(2): 281.
18. Macri, P. P., Enzo, S., Cowlam, N., Frattini, R., Principi, G., & Hu, W. X. (1995). Mechanical alloying of immiscible Cu70TM30 alloys (TM= Fe, Co). *Philosophical Magazine B*, 71(2): 249-259.
19. Yavari, A. R., Desre, P. J., & Benameur, T. (1992). Mechanically driven alloying of immiscible elements. *Physical review letters*, 68(14): 2235-2238.
20. Eckert, J., Holzer, J. C., & Johnson, W. L. (1993). Thermal stability and grain growth behavior of mechanically alloyed nanocrystalline Fe-Cu alloys. *Journal of applied physics*, 73(1): 131-141.
21. Huang, X., & Mashimo, T. (1999). Metastable BCC and FCC alloy bulk bodies in Fe–Cu system prepared by mechanical alloying and shock compression. *Journal of alloys and compounds*, 288(1): 299-305.
22. Drbohlav, O., & Yavari, A. R. (1995). Mechanical alloying and thermal decomposition of ferromagnetic nanocrystalline fcc-Cu50Fe50. *Acta metallurgica et materialia*, 43(5): 1799-1809.
23. Alami, A. H., Alketbi, A., & Almheiri, M. (2015). Synthesis and microstructural and optical characterization of Fe-Cu metastable alloys for enhanced solar thermal absorption. *Energy Procedia*, 75: 410-416.
24. Cullity, B. D. (1956). Elements of X-ray Diffraction. Addison and Wesley Publishing Company Inc. *Reading, USA*: 99.
25. Azabou, M., Gharsallah, H. I., Escoda, L., Suñol, J. J., Kolsi, A. W., & Khitouni, M. (2012). Mechanochemical reactions in nanocrystalline Cu–Fe system induced by mechanical alloying in air atmosphere. *Powder technology*, 224: 338-344.
26. Eckert, J., Holzer, J. C., Krill iII, C. E., & Johnson, W. L. (1993). Mechanically driven alloying and grain size changes in nanocrystalline Fe-Cu powders. *Journal of applied physics*, 73(6): 2794-2802.
27. Crespo, P., Barro, M. J., Navarro, I., Vazquez, M., & Hernando, A. (1995). Magnetic properties of Fe_xCu_{1-x} solid solutions. *Journal of magnetism and magnetic materials*, 140: 85-86.
28. Drbohlav, O., & Yavari, A. R. (1994). Magnetic properties of mechanically alloyed nanocrystalline fcc $Cu_{50}Fe_{50}$ during thermal decomposition. *Journal of magnetism and magnetic materials*, 137(3): 243-248.
29. Orecchini, A., Sacchetti, F., Petrillo, C., Postorino, P., Congeduti, A., Giorgetti, C., Baudelet, F., & Mazzone, G. (2006). Magnetic states of iron in metastable fcc Fe–Cu alloys. *Journal of alloys and compounds*, 424(1): 27-32.